ACOUSTICALLY ENHANCED BOILING HEAT TRANSFER

Marc K. Smith, Steven W. Tillery, Samuel N. Heffington, and Ari Glezer

George W. Woodruff School of Mechanical Engineering
Georgia Institute of Technology
Atlanta, GA 30332-0405

ABSTRACT

Technological advances have increased the demands on thermal management systems in aerospace, microelectronics, and other applications to the point where boiling and multi-phase heat transfer technologies are needed. One popular technology, immersion cooling using pool boiling, is limited by a catastrophic transition from nucleate to film boiling at a well-defined critical heat flux limit. The present work used an acoustic emitter located near the heated surface to actively control the boiling process. When vapor bubbles reached a predetermined size, the acoustic field forced them to detach from the heated surface. This led to an increase in the heat transfer rate and a delay in the transition from nucleate to film boiling. Preliminary work demonstrated acoustically enhanced bubble detachment from a heated surface over a frequency range of kHz to MHz. For water, the critical heat flux limit was increased from 107 W/cm^2 at 122 °C to 299 W/cm^2 at 136 °C. This work also showed that the excitation process is robust enough to work against buoyancy forces, if present. Thus, acoustically enhanced boiling in a closed heat transfer cell has the potential to produce a simple, high performance device that would be attractive for a wide variety of high-heat-flux applications.

INTRODUCTION

In the microelectronics industry, advances in technology have brought about an increase in transistor density and faster electronic chips. As electronic packages increase in speed and capability, the heat flux required to maintain a reasonable chip temperature has also risen. Cooling fluxes are projected to reach the 1000 W/cm^2 level in the next five to ten years for some high power electronic applications such as hybrid vehicles that use power conditioning transistors for electronic motor control and regulation[1].

Two-phase heat transfer involving the evaporation of a liquid in a hot region and the condensation of the resulting vapor in a cooler region can provide the large heat fluxes needed for microelectronic packages to operate at acceptable temperature levels. By changing the phase of the working fluid, a two-phase heat transfer cooling scheme supports high heat transfer rates across moderately small temperature differences. Heat pipes and thermosyphons are examples of efficient heat transfer devices that exploit the benefits of two-phase heat transfer[2–4]. Immersion cooling, which involves the boiling of a working fluid on a heated surface, is another example of a two-phase cooling technology used in microelectronic applications[5].

Immersion cooling is a highly effective cooling strategy for two reasons: 1) the high thermal conductivity of the liquid medium as opposed to that of air enhances natural or forced convection from the heated surface, and 2) the liquid to vapor phase change at higher heat fluxes is an extremely effective means for heat removal. Recently, interest in liquid immersion coolers has increased because of the need for effective cooling in microelectronic devices as described in the review by Bar-Cohen[6]. The performance of an immersion cooler at the high heat fluxes required of present and future applications is possible because of the nucleate boiling that occurs with direct liquid contact on the heated surface. Boiling heat transfer has been widely studied for the last fifty years and has been reviewed by many authors, e.g., Dhir[7]. A key reason for the efficient heat transfer that occurs during boiling is that buoyancy forces remove the vapor bubbles generated at the heated surface. When the heat flux from the surface is increased past a critical level of 126 W/cm^2 for water at standard conditions, a large, possibly catastrophic increase in surface temperature occurs. This critical heat flux marks the transition from nucleate boiling to film boiling. In film boiling, a thin layer of vapor completely covers the heated surface. The vapor layer insulates the surface and thus causes the large temperature increase at the same heat flux. This boiling transition occurs at much lower heat fluxes in a microgravity environment because buoyancy forces are almost negligible. Thus, the performance of immersion cooling in microgravity is drastically reduced.

Within the past fifty years, much research has been conducted in the area of jet impingement heat transfer. Comprehensive reviews of this topic are presented by many authors, including Downs and James[8], Hrycak[9], and Martin[10]. Investigations conducted by Ma *et al.*[11–12] demonstrated heat fluxes as high as 280 W/cm^2 at a wall temperature of 58 °C by impinging a microelectronic device with a two-phase, two-component jet. By impinging a submerged heated surface with a jet, the onset of critical heat flux can be substantially delayed. Initial work conducted by Katto and Monde[13] showed how the onset of critical heat flux during boiling for a heated surface being impinged by a jet was directly related to the velocity of the jet.

In the present work, a new design for an immersion cooling cell is presented that combines jet impingement onto the heated surface with a small cross flow in the cell. The jet developed and utilized in this device is formed by oscillating cavitation bubbles present on the surface of a submerged vibrating piezoelectric diaphragm operating at or near resonance. Direct impingement of this jet onto the heated surface in the cell forcibly removes vapor bubbles from the surface. The small cross flow moves the bubbles away from the surface so they can condense in the bulk liquid and allows the heated surface to be rewetted with incoming cooler bulk liquid. By coupling these two heat transfer enhancement techniques into a single heat transfer cell, the critical heat flux was greatly increased. Because of this, a heat transfer cell based on the vibration-induced jet technology removes a larger heat flux for a given surface temperature than other immersion coolers.

The remainder of this paper is organized as follows. A flow visualization of the vibration-induced jet and how it will be used in the cooling cell is presented in the next section. Then, the design of the cooling cell is discussed followed by the results from the heat transfer studies on this cell. In the final section, we summarize the results and conclude.

FLOW VISUALIZATION

For visualization purposes, a vibration-induced jet was produced by an actuator composed of a vibrating circular diaphragm mounted to a fixed surface and submerged in a water tank. A photograph of the jet is shown in Fig. 1. The jet was visualized by a streak of dye entrained radially from an injection port near the edge of the diaphragm above the jet. As discussed by James *et al.*[14], the vibration-induced jet has finite linear streamwise momentum, but, in contrast to conventional jets, it is formed without net mass injection into the liquid and is composed entirely of axisymmetrically entrained fluid. When the oscillation amplitude of the diaphragm surpassed a given threshold, the jet appeared near the center of the diaphragm along with a small cluster of cavitation bubbles. Pressure oscillations due to the diaphragm's motion resulted in the time-periodic formation and collapse of these cavitation bubbles, which then entrained surrounding liquid and generated the turbulent jet directed normal to the surface of the diaphragm and flowing away from its center. The jet Reynolds number in this visualization was approximately 2000, based on a jet diameter equal to the characteristic diameter of the cavitation bubbles (approximately 2 mm) and a streamwise average velocity near the bubbles of approximately 1 m/s.

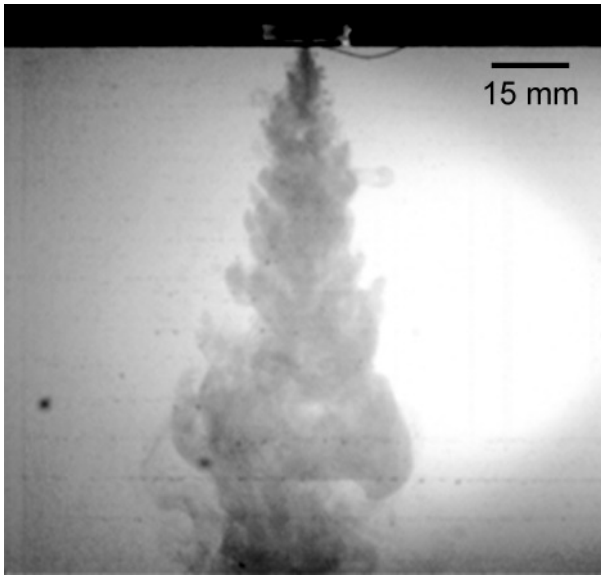

Figure 1: Dye visualization photograph of a turbulent vibration-induced jet. The dye was entrained radially from an injection port near the edge of the diaphragm.

Even though a vibration-induced jet results from time-periodic excitation, the time-averaged jet structure is very similar to that of a conventional round turbulent jet. According to James *et al.*[14], the jet appears to become turbulent at or near the surface of the diaphragm. The jet diameter increases linearly and the centerline velocity decreases linearly with the streamwise distance from the diaphragm. Also, the mean flow of the jet exhibits a remarkable tendency toward self-similarity as has been extensively documented for higher Reynolds number conventional jets, e.g., Rajaratnan[15].

EXPERIMENTAL APPARATUS

A photograph of the heat transfer cell used in this work is shown in Fig. 2. The cell was machined from a solid block of Lexan measuring 51 mm wide, 25 mm high, and 76 mm long. The internal dimensions of the cell were 46 × 18 × 48 mm. In order to control the fluid temperature within the cell, a small cross flow was used. This was done by installing a 1/4 NPT fitting into each end of the cell. Using these fittings, subcooled water was supplied to the cell from a chilled water bath. This was done in such a way as to allow the water temperature and the flow rate into the cell to be independently varied.

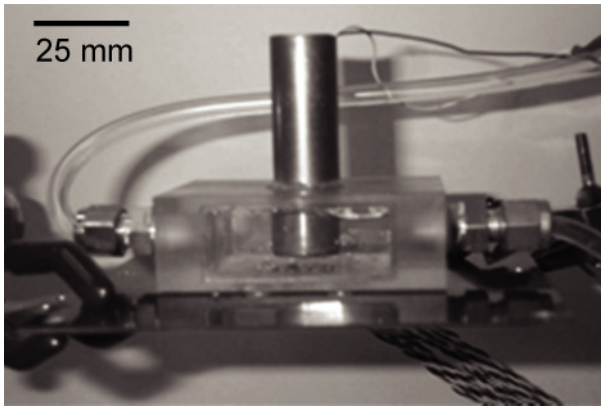

Figure 2: A photograph of the vibration-induced jet, heat transfer cell. The front and rear sides were fitted with an acrylic sheet to provide an unobstructed view inside the cell.

The actuator used to produce the vibration-induced jet was composed of a circular brass diaphragm with a diameter of 18.2 mm and a thickness of 0.39 mm driven by a concentrically mounted piezoceramic wafer with a diameter of 11.6 mm and a thickness of 0.19 mm. The diaphragm was glued to the end of a 5 cm long brass tube with an inner diameter of 17.5 mm. The tube was inserted and glued into a 19 mm hole drilled into the top of the cell so that the actuator was at a fixed distance and parallel to the heated surface. The actuator was driven at the resonance frequency of its first axisymmetric mode of vibration (nominally 7 kHz) using a laboratory function generator and a high voltage (max. 120 V_{rms}) broadband (25 Hz–150 kHz) amplifier. In order for the jet to form, the driving voltage had to be large enough so that the surface of the vibrating piezoelectric diaphragm exceeded a threshold acceleration of 3300 g and a threshold displacement of 12 μm[16]. When the jet formed, it flowed in a normal direction to the surface of the submerged actuator and impinged normally on the heated surface. A simple sketch of the actuator showing the formation of the vibration-induced jet and its interaction with the vapor bubbles on the heated surface in the cell is shown in Fig. 3.

Understanding the conditions required to produce the jet was crucial to the development of a heat transfer cell based on the vibration-induced jet technology. Insufficient driver acceleration or displacement would allow vapor bubbles to completely insulate the heated surface leading to catastrophic dry out. Operating above the threshold acceleration and displacement levels ensured the continual operation of the jet.

In this particular cell design, the open end of the brass tube attached to the vibrating diaphragm was unshielded outside of the cell (see Fig. 2). Thus, the acoustic emissions from the diaphragm when a jet was present were greater than 90 dBA. In order to use this technology in most microelectronic cooling applications, reducing the noise level to acceptable limits presents a significant challenge.

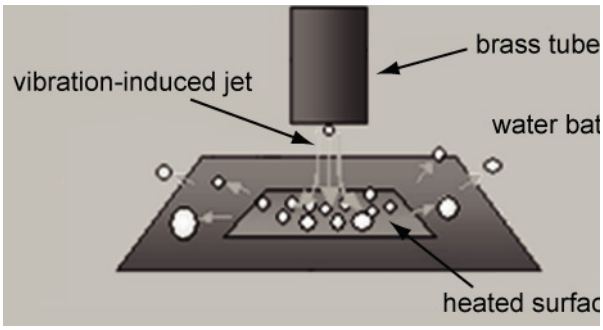

Figure 3: A sketch of the vibration-induced jet removing vapor bubbles from the heated surface in the cell.

The diaphragm was positioned inside the cell at a separation distance from the heated surface of 5.7 mm. This was the distance for optimal heat transfer enhancement resulting from direct impingement by the vibration-induced jet during pool boiling as reported previously by Glezer *et al.*[16]. If the actuator surface was closer than 5.7 mm, vapor bubbles generated by the heated surface often

coalesced and bridged the gap between the actuator and the heated surface forming a vapor bridge that resulted in temperature runaway due to dryout. Separation distances larger than 5.7 mm resulted in decreased jet momentum due to viscous losses and therefore, decreased heat transfer performance for the cell.

The heat transfer cell was designed to allow the use of two different heating elements: a thermal test die and a calibrated copper heater. The cell could be mounted to each heater in such a way as to align the center of the heated surface with the center of the diaphragm while exposing the entire heated surface to the water within the cell.

The thermal test die is an industry standard test device. It was designed to simulate a desktop microprocessor chip and produces a uniform heat flux on the chip's surface. When mounting the die to the heat transfer cell the heat-spreader lid was removed so that the surface of the chip was exposed to the water in the cell. The power delivered to the die was measured by monitoring the applied steady-state voltage and current levels. The heat flux removed from the chip's surface was estimated by dividing the total power delivered to the die by the exposed surface area of the chip (1.18 cm^2). The temperature of the chip's surface was measured using temperature sensors embedded within the die. Standard uncertainty analysis determined that the heat-flux measurements from the die were accurate to within 5% and the surface temperature was accurate to within ±0.5 °C.

A calibrated copper heater was used to access higher values of the surface heat flux and surface temperature (>115 °C) than were possible with the thermal test die. The heater was approximately 51 mm long. The lower section of the heater was a cylinder 22.23 mm in diameter containing a resistance heater powered by a 110 V voltage regulation unit. A short tapered section brought the diameter down to 14.14 mm. The final 10 mm of the heater had a square cross section with an area of 1.0 cm^2. The square end of the heater was pushed through an insulating board and its upper surface was flush mounted to the inside lower surface of the heat transfer cell. The heater was heavily insulated so that one-dimensional heat conduction was attained in the upper square section of the heater. Three levels of three thermocouples were imbedded within this square section at 3.18 mm intervals beginning 3.18 mm from the heater's upper surface. From these temperature measurements, the heat flux was computed as the thermal conductivity multiplied by the temperature difference divided by the distance separating the thermocouples. The temperature of the heater's upper surface was linearly extrapolated from the thermocouple measurements. Standard uncertainty analysis determined that the heat-flux measurements from this heater were accurate to within 7% and the extrapolated surface temperature was accurate to within ±1.0 °C.

The experimental procedure for each of the experiments was as follows. First, the water used in the bath was preheated to 60–80 ºC for more than two hours before the experiment was performed in order to remove as much dissolved air as possible. After degassing, the bath water temperature was quickly chilled to the desired cell inlet temperature. The hoses from the chilled water bath were then connected to the cell, the cell filled with water, and all visible air bubbles were removed so that a steady flow was established. Next, for those cases in which a vibration-induced jet was used, the actuator was energized with approximately 90 V_{rms} to form the jet. In each test, the heater was then powered up in small voltage increments. For each increment, the

surface temperature of the heater was allowed to reach steady state before it was recorded along with the corresponding heat flux. For the thermal test die, the test was terminated when the surface temperature of the chip was 115 °C, 5 °C lower than the maximum allowable value of 120 °C. For the calibrated copper heater, the test was terminated when the average temperature from the three thermocouples embedded within the heater was approximately 200 °C. This temperature limit was chosen so as not to exceed the accuracy range of the thermocouples.

EXPERIMENTAL RESULTS

THERMAL TEST DIE

In the first experiment, the water temperature at the cell inlet was 20 °C and the flow rate was fixed so that the average velocity of the flow in the cell was 15 mm/s. Data was collected for channel boiling with the jet on and off. A series of photographs depicting the effect of the vibration-induced jet is shown in Fig. 4. Without the jet, the cross flow within the cell did little to remove the insulating vapor bubbles from the surface of the test die. When the jet was turned on, these vapor bubbles were swept away from the surface in 0.1 s.

The heat flux from the surface of the die to the water versus the die surface temperature is shown in Fig. 5 (open symbols). With no jet and a surface temperature of 111 °C, the heat flux was 35.5 W/cm^2. With the jet on, the heat transfer was much more significant. Below a die temperature of 100 °C (the onset of boiling) the presence of the jet increased the heat flux for a given temperature. The turbulent jet provided additional forced convection heat transfer from the die to the flowing water within the cell. The added turbulent mixing and bulk motion present when the jet was on compared to the very small amount of forced convection heat transfer when the jet was off resulted in higher heat fluxes. Above 100 °C, the jet removed the insulating vapor bubbles from the surface of the die, as shown in Fig. 4. As a result of this, the heat flux as a function of surface temperature increased at a faster rate. While the cross flow alone had little effect on the heat flux from the surface, the cross flow coupled with the jet worked together to

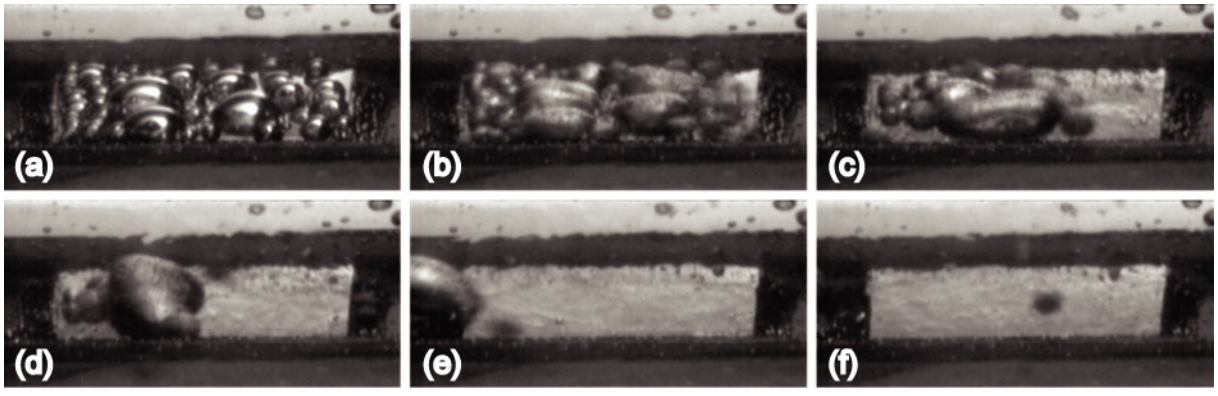

Figure 4: A visualization of the vibration-induced jet removing vapor bubbles from the surface of the thermal test die. Photographs (a – f) were taken at 0.02 s intervals for a total duration of 0.1 s.

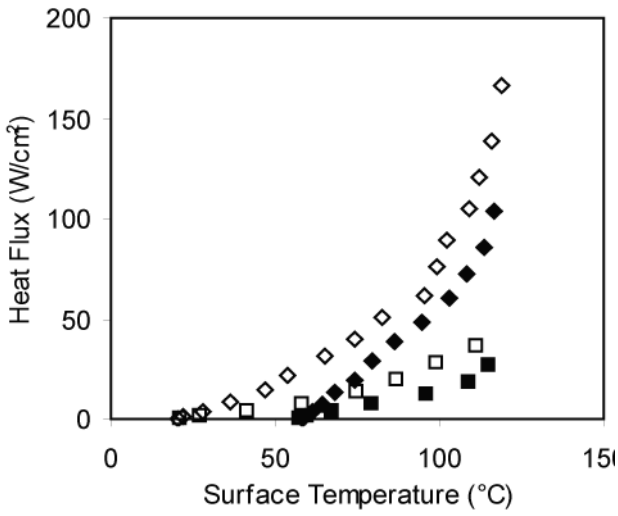

Figure 5: The effect of direct impingement by the vibration-induced jet on the heat flux from the die surface for an inlet water temperature of 20 °C (open symbols) and 60 °C (filled symbols). Jet off (squares) and jet on (diamonds).

sweep the removed vapor bubbles downstream where they condensed. In addition to this, the cross flow provided cooler water to the jet that increased the heat transfer due to the forced convection of the jet on the die surface. The data from Fig. 5 shows that at a surface temperature of 111 °C, the direct impingement of the jet onto the die surface increased the heat flux from the surface to 116 W/cm^2, a 227% improvement over the case with no jet (35.5 W/cm^2). This was a result of the jet increasing the overall heat transfer coefficient through increased convection and the removal of the insulating vapor bubbles. These effects also increased the critical heat flux limit to 166 W/cm^2 at a temperature of 119 °C.

In the next experiment, also shown in Fig. 5 (filled symbols), the flow rate was the same as before but the water temperature at the cell inlet was increased to 60 °C. The increase in the water temperature decreased the heat transfer for both the convective range ($T < 100$ °C) and the boiling range ($T > 100$ °C). The data from Fig. 5 shows that at a surface temperature of 111 °C, the heat transfer from the die surface increased from 20.6 W/cm^2 to 78.6 W/cm^2, a 282% improvement. This improvement in heat transfer was even greater that when the cell inlet temperature was 20 °C. This is attributed to the fact that the strength of the jet remained virtually constant at the two bath temperatures, while the surface heat flux during boiling with no jet decreased as the temperature of the water in the bath increased. Thus, the jet provided a greater overall improvement in heat transfer for the higher bath temperature. In this experiment, the jet also increased the critical heat flux limit to 104 W/cm^2 at a temperature of 117 °C.

CALIBRATED COPPER HEATER

The purpose of this heater was to establish the vibration-induced jet's ability to increase the heat flux from a heated surface at surface temperatures greater than 115 °C. For these experiments, the inlet temperature of the water to the cell was set to a constant 20 °C and the flow rate of the water bath was set so that the average velocity of the water in the cell was 15 mm/s. Tests were conducted with the heat transfer cell in a horizontal orientation and rotated 45° with respect to the horizontal so that the cell inlet was located below the cell outlet. For all cases, data was collected for channel boiling with the jet on and off. The results are shown in Fig. 6. The first case examined was the horizontal cell. When the surface temperature of the calibrated heater was approximately 120 °C, the influence of the jet on the heat flux from the heater's surface was at its maximum. As the surface temperature of the calibrated heater approached 150 °C, the influence of the jet decreased to a point where the jet had no influence on the surface heat flux.

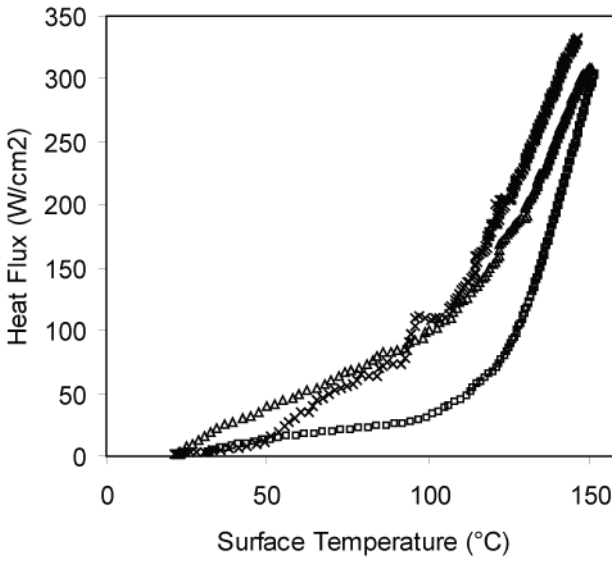

Figure 6: The effect of inclining the heat transfer cell by 45° to the horizontal. Horizontal cell with no jet (□), horizontal cell with a jet (△), and inclined cell with a jet (x).

When the cell was inclined to 45°, the influence of the jet did not become minimal until a much higher surface temperature. Because of this, a heat flux of over 350 W/cm^2 was attained before the jet no longer influenced the surface heat flux.

In an inclined heat transfer cell, buoyancy caused the vapor bubbles to move upward toward the cell outlet, particularly at the higher surface temperatures. With this added assistance, the jet was able to remove bubbles from the heated surface at temperatures higher than what was attainable in a horizontal cell. Also in the horizontal orientation, the jet was strong enough to expel the heated water from the heated surface in all directions, including upstream of the heater. Because of this, the jet was provided with increasingly warmer water to impinge onto the heated surface, which decreased the heat transfer. In an inclined cell, the heated water being expelled from the heater moved almost entirely downstream of the heater. Thus, cooler water was supplied to the jet, which increased the heat transfer. Both of these mechanisms contributed to the overall increase in the heat transfer from the heated surface as the inclination angle of the cell increased. Since the mechanism for this increase in heat transfer is buoyancy, the optimum inclination angle is most likely 90°. However, the experiments needed to determine the optimum cell inclination angle were not performed.

CONCLUSIONS

A heat transfer cell based on a new, vibration-induced jet technology has been demonstrated and tested. In this technology, a piezoelectric diaphragm was used to produce a submerged turbulent jet that was directed at both a microelectronic test die as well as a calibrated copper heater. The jet had enough momentum to remove the vapor bubbles that formed on both heaters during channel boiling. The bubbles moved into the cooler bulk liquid and the cross flow within the cell swept them downstream where they condensed. Heat fluxes up to 166 W/cm^2 at a surface temperature of 119 °C were achieved in a compact geometry requiring approximately 1 W of input power. For channel boiling at a surface temperature of 111 °C, the jet increased the heat flux from the heated surface by 226%. When the cell inlet temperature was increased from 20 °C to 60 °C, the jet increased the heat flux by 282%.

Using the calibrated heater as the heat source, it was shown that the greatest amount of improvement in heat flux for a given surface temperature occurred near 120 °C. Beyond this point, the effectiveness of the jet declined until the surface temperature of the heater approached 150 °C and the surface heat flux was approximately 300 W/cm^2. Above this temperature, the jet

had minimal effect on the heat transfer. By inclining the heat transfer cell 45° to the horizontal so that the water inlet was positioned below the water outlet, the influence of the jet did not become minimal until a much higher surface temperature was achieved. Because of this, a heat flux of over 350 W/cm^2 was attained before the jet no longer influenced the heat flux from the surface of the heater.

ACKNOWLEDGMENT

This work was supported by the NASA Microgravity Research Program under Grant NAG3-2763.

REFERENCES

1. Zerby, M. and M. Kuszewski, "Final Report on Next Generation Thermal Management (NGTM) for Power Electronics," NSWCCD Technical Report TR-82-2002012 (2002).

2. Peterson, G. P., "An Introduction to Heat Pipes," John Wiley & Sons, Inc., New York, pp. 285–326 (1994).

3. Kiewra, E. W. and P. C. Wayner, "A Small Scale Thermosyphon for Immersion Cooling of a Disc Heat Source," Heat Transfer in Electronic Equipment, ASME Symposium HTD-Vol. 57, Bar-Cohen, A. (Ed.), American Society of Mechanical Engineers, New York, pp.77–82 (1986).

4. Mudawar, I., T. A. Incropera, and F. P. Incropera, "Microelectronic Cooling by Fluorocarbon Liquid Films," Proc. Int. Symposium of Cooling Technology for Electronic Equipment (1987).

5. Arik, M. and A. Bar-Cohen, "Immersion Cooling of High Heat Flux Microelectronics with Dielectrid Liquids," 4th Int. Symposium and Exhibition on Advanced Packaging-Materials-Processes-Properties, Atlanta, pp. 229–247 (1998).

6. Bar-Cohen, A., "Thermal Management of Electronic Components With Dielectric Liquids," JSME Int. J. 36, pp. 1–25 (1993).

7. Dhir, V. K., "Boiling Heat Transfer," Ann. Rev. Fluid Mech. 30, pp. 365–401 (1998).

8. Downs, H. T. and E. H. James, "Jet Impingement Heat Transfer – A Literature Survey", ASME Paper, 87-HT-35 (1987).

9. Hrycak, P., "Heat Transfer From Impinging Jets – A Literature Review," Technical Report AFWAL-TR-81-3504, Flight Dynamics Laboratory, Wright Patterson AFB, Ohio (1981).

10. Martin, H., "Heat and Mass Transfer Between Impinging Gas Jets and Solid Surfaces," Advances in Heat Transfer 13, pp. 1–60 (1977).

11. Ma, C. F. and Y. Q. Tian, “Experimental Investigation on Two-Phase Two-Component Jet Impingement Heat Transfer from Simulated Microelectronic Heat Sources,” Int. Comm. Heat Mass Transfer 17, pp. 399–408 (1990).

12. Ma, C. F. and A. E. Bergles, “Boiling Jet Impingement Cooling of Simulated Microelectronic Chips,” ASME, HTD-Vol. 28, pp. 5–12 (1983).

13. Katto, Y. and M. Monde, “Study of Mechanism of Burn-Out in a High Heat-Flux Boiling System with an Impinging Jet,” Int. Heat Transfer Conference 4, pp. 245–249 (1974).

14. James, R. D., J. W. Jacobs, and A. Glezer, “A Round Turbulent Jet Produced by an Oscillating Diaphragm,” Phys. Fluids 8, pp. 2484–2495 (1996).

15. Rajaratnan, N., “Turbulent Jets,” Elsevier Scientific, New York (1976).

16. Glezer, A., S. Heffington, M. Smith, S. Tillery, “Enhanced Boiling Heat Transfer by Submerged, Vibration Induced Jets,” 9th Therminic Conference, Aix-en-Provence, France, Sept. 24–26 (2003).

CONTACT

Marc K. Smith, Professor
George W. Woodruff School of Mechanical Engineering
771 Ferst Drive NW
Georgia Institute of Technology
Atlanta, GA 30332-0405
Phone: 404-894-3826 Fax: 404-894-8496
Email: marc.smith@me.gatech.edu